

## REFRATÁRIOS PARA FORNO ELÉTRICO A ARCO DE PIROMETALURGIA DE CONCENTRADO DE NIÓBIO. \*

*Alaércio Salvador Martins Vieira<sup>1</sup>*

### **Resumo**

Considerações técnicas sobre refratários utilizados em forno elétrico a arco, para refino de concentrado de nióbio estão descritas neste artigo. Propriedades de diversos tijolos, divididos em dois grupos, refratários óxidos e carbono-óxidos foram estudados. Considerando a resistência a corrosão em função da composição química, as propriedades de cada tipo de tijolo estão descritas, com relação a seu comportamento em serviço. De acordo com os experimentos, melhores resultados podem ser obtidos utilizando tijolos neutros de carbono-óxidos. É importante salientar que em aplicações industriais outras variáveis podem atuar, tais como, refrigeração de carcaça, operação com arco aberto ou submerso, operação contínua ou em batelada e atmosfera de gases do forno.

**Palavras-chave:** Refratários; Pirometalurgia, Óxidos, Carbono.

## REFRACTORIES FOR ELETRIC ARC FURNACE OF PIROMETALURGY OF NIOBIUM CONCENTRATE.

### **Abstract**

Technical considerations about refractories to electric arc furnace of refined niobium concentrate production are presented in this paper. Properties of several bricks, divided in two groups, oxides and oxide-carbon refractory, have been studied. Taking into account the slag chemical corrosion resistance, the properties of each brick are showed regarding its behavior in service. According to experiments, better lifetime might be achieved in using neutral oxide-carbon bricks. It is important to remember that, in industrial application other circumstances must be related, such as, water-cooling, open or submerged arc, continuous or batch operation and atmosphere conditions.

**Keywords:** Refractories, Pyrometallurgical, Oxide-carbon.

<sup>1</sup> *Metallurgical Engineer, Materials Engineering Specialist, ATR Metals Consulting, Araxá, Minas Gerais, Brazil.*

## 1. INTRODUCTION

CBMM, Companhia Brasileira de Metalurgia e Mineração, is the main niobium producer in world. Its annual production is about 81.000 short tons of all products, standard ferroniobium, high purity ferroniobium, nickel niobium, high purity niobium oxide, optical grade niobium oxide and niobium metal (commercial and reactor grade). Its industrial site is located in Araxá, Minas Gerais State, and there are three subsidiaries, CBMM Europe (Amsterdam), CBMM Asia (Singapore) and CBMM North America (Pittsburgh). In the standard ferroniobium process route there is a Pyrometallurgical step, which uses two electric arc furnaces (EAF) to remove Phosphorus and prepares the concentrate to an aluminothermic reduction. Table 1 shows furnace details, describing an operational range and construction dimensions, as well. CBMM and Magnesita SA have been working together in order to increase the refractory work-line performance, testing refractories compatible with operational temperature, chemical composition and safety requirements.

**Table 1.** Details of furnaces

Furnace	Short ton/day	Operating temperature	Dimensions (inch)
1 and 2	265	1623 to 1823K	Furnace = 170 height x 189 diameter Reaction shaft = 39 height x 189 diameter

Source: CBMM

Figure 1 represent a schematic description of refractories. The work-line bricks have larger thickness than an inwall bricks. Both EAF are 10.5 MVA.

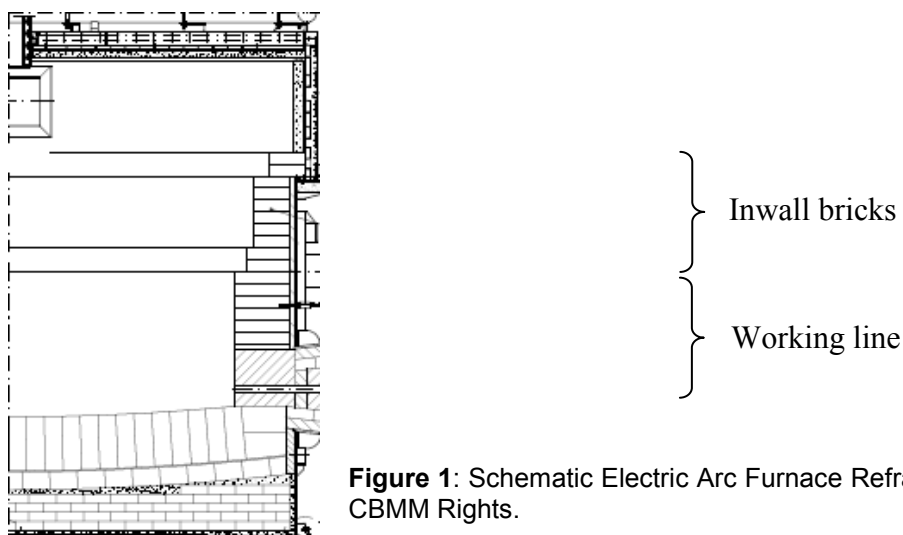


**Figure 1:** Schematic Electric Arc Furnace Refractory view. Source: CBMM Rights.

### 1.1 PYROMETALLURGICAL PROCESS

The Pyrometallurgical process develop by CBMM has been in operation whether 2000. This process is unique to niobium production in the word, and represents a new step, regarding cost savings, improvements in quality, environmental protection and human occupation safety. Pyrometallurgical

process for niobium concentrated is carried out in two complementary stages, Sintering and Electric Arc Furnace smelting.

Initially, the floated concentrate is pelletized with a carbon source and silica binding material. Then, poured into a belt-sintering furnace, designed by Outokumpu Oy. This process removes sulphur, moisture, and prepares the niobium concentrate to a smelting process, as well. Table 2 reports an average chemical analysis of process.

**Table 2:** Analysis of floated and sinter concentrated

Typical Sample	% C	% H <sub>2</sub> O	% Nb <sub>2</sub> O <sub>5</sub>	% S
Belt-sintering Furnace Feed	0.49	10.00	50.00 to 54.00	0.14
Sintered Niobium Concentrate	0.06	0.10	54.00 to 58.00	0.01

Source: CBMM

Sinter concentrate is charged in the EAF, designed by SMS Demag, by scaling feed belts. During the sinter feeding another carbon source, and ironscrap might be loaded to promote a suitable charge composition. Carbon reduces phosphorous and lead oxides. Fumed lead reoxidises in the furnace atmosphere or in the exhaustion hood being collected as powder in bag-houses filter. Iron metal, or Fe<sub>2</sub>O<sub>3</sub> from sinter concentrate, combines with reduced phosphorous and forms a ferro-phosphorous alloy (FeP), as simplified equation below and presented in table 3 regarding chemical composition.



**Table 3:** Analysis of FeP Alloy

Typical	% C	% S	%Pb	% P	% Fe
Ferro Phosphorous Alloy	0.15	0.01	< 0.15	10.00 to 15.00	80.00 to 85.00

Source: CBMM

During carbothermicreaction, refined niobium concentrate and the FeP alloy separate from the charge due to its differentmass densities. The highest density liquid (metal phase) goes down to bottom, and the oxide phasegoes to upper layer. The range of process temperature is 1623 to 1823K. When all the charge is already molted and ends the phase segregation, the niobium concentrate, now renamed as Refined Concentrate is tapped from the EAF to a water granulation system. Smelting process takes place around3 hours.

**Table 4:** Analysis of Refined Niobium Concentrate

Typical Sample	% Nb <sub>2</sub> O <sub>5</sub>	% Fe <sub>2</sub> O <sub>3</sub>	% SiO <sub>2</sub>	% P	% S	% C
Refined Concentrate	60.00 to 63.00	3.40	1.34	0.129	0.007	0.005

Source: CBMM

After water granulation, the refined concentrate is filtered in a vacuum belt filter, dried in a gas-fired kiln and finally packaged. Table 4 reports elements with outstanding importance to the next metallurgical reduction process. The FeP alloy is tapped when reaches a certain level in the molten batch, avoiding to be leaked out at the concentrate drain hole.

## 1.2 REFRACTORIES TO PIROMETALURGY OF NIOBIUM CONCENTRATE

Refractories have been studied regarding their chemical and physical properties in order to investigate the correlation between properties, operational conditions and chemical composition. The refractories were divided in oxides and oxide-carbon refractories groups, according tables 5 e 6, which show common compositions.

Another approach that needs to be taken into account is the classification of these materials as their chemical composition. Acid refractories are commonly used in areas where slag and atmosphere are both acidic. They are stable towards acids but attacked by alkalis. The main raw materials belong to RO<sub>2</sub> group, silica (SiO<sub>2</sub>) and zirconia (ZrO<sub>2</sub>)<sub>Ref. (3)</sub>.

Neutral Refractories are ordinarily used in areas where slag and atmospheres are either acidic or basic, and are chemically stable to both acids and bases. The main raw materials belong, but not exclusively, to the group R<sub>2</sub>O<sub>3</sub>. Examples of these materials are corundum (Al<sub>2</sub>O<sub>3</sub>), chromia (Cr<sub>2</sub>O<sub>3</sub>) and carbon<sub>Ref. (1)</sub>.

Basic refractories are usually used in areas where slag and atmosphere are both basic. They are stable in alkaline environments, but they react with acids. The main raw materials belong to the group RO, and periclase (MgO) is a known example. Other examples include dolomite and periclase-chromia<sub>Ref. (2)</sub>.

**Table 5:** Chemical analysis of pure oxides bricks ( % )

Brick	Al <sub>2</sub> O <sub>3</sub>	SiO <sub>2</sub>	TiO <sub>2</sub>	Fe <sub>2</sub> O <sub>3</sub>	Na <sub>2</sub> O+K <sub>2</sub> O	MgO	Cr <sub>2</sub> O <sub>3</sub>	CaO	ZrO <sub>2</sub>
Specimen 1 (CM)	79.0 / 83.0	15.0 max	4.0 max	2.0 max	0.4 max	-	-	-	-
Specimen 2 (PM)	-	-	-	-	-	96.5 / 98.5	-	-	-
Specimen 3 (PCr)	6.8	1.1	-	7.3	-	66.4	17.4	0.6	-
Specimen 4 (SP)	12	0.3	-	0.5	-	84	-	0.8	1.8
Specimen5 (CCZ)									

Source: Magnesita SA

**Table 6:** Chemical analysis of oxide-carbon bricks ( % )

Brick	Al <sub>2</sub> O <sub>3</sub>	MgO	SiO <sub>2</sub>	Total Carbon	SiC
Specimen6 (CCb)	86.1	-	4.5	15.4	6.3
Specimen7 (PCb)	-	92.5	-	12.0	-
Specimen8 (GP)	-	-	-	100	-

Source: Magnesita SA

## 1.3 EXPERIMENT PROCEDURE

The hole of a slag corrosion or dissolution resistance experiment is measure the resistance to the attack by slag or molten metal at the refractory linings. It is possible to compare wearing and the mineralogical phases present. The Research Center of Magnesita SA has two induction furnaces, and uses a standard procedure, as follows:

$$DLE = \frac{\frac{[(MI - 1) + (MI - 2)]}{2} - \frac{[(MFE - 1) + (MFE - 2)]}{2}}{(MI - 1) + \left(\frac{MI - 2}{2}\right)}$$

DLE: Corrosion at the slag line

MI-1: Initial thickness at the hot surface, relative to upper brick.

MI-2: Initial thickness at the hot surface, relative to central brick.

MFE-1 e MFE-2: Final thicknesses at the hot surface, relative to slag line.

Bricks were prepared in specimens, 6.3 x 1.57 x 1.57 inch<sup>3</sup>, to design a lining to electromagnetic induction furnace. The corrosion resistance test was carried out assembling eight specimens, 2 for each type of composition, filling out the crucible. Metallic charge was added as a source for liquid metal, approximately 4.41 pounds of steel SAE1020 and about 17.64 pounds of FeP alloy to saturate the liquid metal in phosphorus, preventing the reduction of phosphorus oxide on slag. Figure 2 also shows a dissolution mechanism.

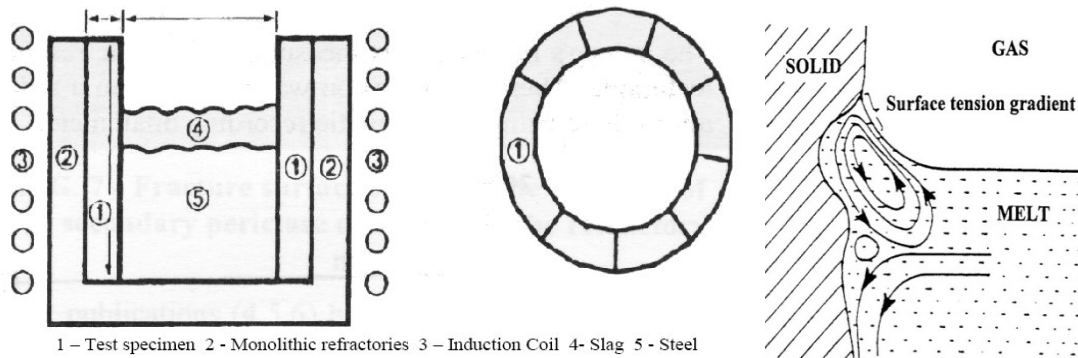


Figure 2: Corrosion resistance test in induction furnace. Source Magnesita SA.

After all metallic charge melted, were added 0.55 pound of granulated slag, which were replaced every 30 minutes, for a total period of 120 minutes. Despite operational temperature range, experimental temperature was increased to 1923K, in order to accelerate the corrosion, facilitating technical measurements and discussions. The experiment follows the sequence of table 7, which was divided in oxides and oxide-carbon refractories groups.

**Table 7:** Experimental schedule

Test	Brick	Temperature (K)	Slag
1	SpecimenCCb	1923K	Typical
	SpecimenCCZ		
	SpecimenPCb		
	SpecimenGP		
2	SpecimenPM	1923K	Typical
	SpecimenCM		
	SpecimenSP		
	SpecimenPCr		
3	SpecimenCCb	1823K	Typical
	SpecimenCCZ		
	SpecimenPCb		
	SpecimenGP		

**Table 7:** Experimental schedule (continuation)

4	Specimen PM	1823K	Typical
	Specimen CM		
	Specimen SP		
	Specimen PCr		
5	Specimen CCb	2023K	Typical
	Specimen CCZ		
	Specimen PCb		
	Specimen GP		
6	Specimen PM	2023K	Typical
	Specimen CM		
	Specimen SP		
	Specimen PCr		
7	Specimen CCb	1823K	Rich in (P <sub>2</sub> O <sub>5</sub> ) and (PbO)
	Specimen CCZ		
	Specimen PCb		
	Specimen GP		

Source: Author

## 2. RESULTS

Results are showed on tables 8 to 14. It is important to state that all runnings were carried out at the same experimental time, being 2 hours in total. There were no previous ordinations for experiments. Therefore, they were conducted as soon as the linings were available.

Trial temperature varied slightly, according to operational and heating conditions. Graphite took place only in the third experiment, because the third one came first up, and graphite was readily attacked under experimental conditions at the metal-line. In order to guarantee safety procedures and protect the induction furnace, PCb specimens replaced Graphite.

**Table 8:** Running #1

Average temperature = 1929K Steel 1020 and FeP alloy, 17.63lb	CCb	CCZ	PCb
Metal-line corrosion (%)	3.83 1.82	1.98 2.41	2.47 / 1.97 2.10 / 2.83
Slag-line corrosion (%)	16.95 17.49	10.73 10.98	20.56 / 21.01 27.86 / 22.65
inch/h (slag-line)	0.099 0.102	0.064 0.066	0.122 / 0.123 0.165 / 0.133

Source: Author

**Table 9:** Running #2

Average temperature = 1933K Steel 1020 and FeP alloy, 20.96lb	PM	CM	SP	PCr
Metal-line corrosion (%)	11.57 8.08	7.04 7.29	17.68 15.12	15.45 14.76
Slag-line corrosion (%)	33.51 36.23	21.78 24.75	39.79 38.36	35.88 35.49
inch/h (slag-line)	0.204 0.213	0.132 0.146	0.234 0.227	0.212 0.210

Source: Author

**Table 10:** Running #3

Average temperature = 1832K Steel 1020 and FeP alloy, 19.88lb	CCb	CCZ	PCb	GP
Metal-linecorrosion (%)	1.86 2.11	2.74 2.41	2.44 2.32	<b>37.91</b> <b>43.29</b>
Slag-linecorrosion (%)	15.73 15.69	12.12 11.55	27.23 26.12	16.68 16.34
inch/h (slag-line)	0.092 0.092	0.073 0.069	0.159 0.152	0.097 0.095

Source: Author

**Table 11:** Running #4

Average temperature = 1833K Steel 1020 and FeP alloy, 20.55lb	PM	CM	SP	PCr
Metal-line corrosion (%)	7.32 5.85	26.10 14.01	6.68 6.26	7.14 8.72
Slag-linecorrosion (%)	30.82 31.93	21.52 26.13	29.00 27.67	31.00 28.69
inch/h (slag-line)	0.177 0.188	0.126 0.154	0.170 0.163	0.184 0.168

Source: Author

**Table 12:** Running #5

Average temperature = 2029K Steel 1020 and FeP alloy, 17.63lb	CCb	CCZ	PCb
Metal-linecorrosion (%)	2.35 3.23	2.42 3.43	2.37 / 2.28 3.10 / 2.95
Slag-linecorrosion (%)	21.42 21.96	17.56 17.48	31.76 / 34.67 36.27 / 34.53
inch/h (slag-line)	0.126 0.129	0.104 0.104	0.187 / 0.205 0.213 / 0.203

Source: Author

**Table 13:** Running #6

Average temperature = 2033K Steel 1020 and FeP alloy, 20.43lb	PM	CM	SP	PCr
Metal-linecorrosion (%)	13.44 12.56	29.30 29.79	19.48 20.27	15.12 19.54
Slag-linecorrosion (%)	35.68 35.21	48.41 47.92	50.74 51.11	48.81 48.44
inch/h (slag-line)	0.195 0.207	0.286 0.282	0.298 0.301	0.288 0.287

Source: Author

**Table 14:** Running #7

Average temperature = 1928K Steel 1020 and FeP alloy, 18.74lb Slag rich in P <sub>2</sub> O <sub>5</sub>	CCb	CCZ	PCb
Metal-linecorrosion (%)	3.53 2.61	2.78 2.81	2.37 / 3.14 2.73 / 1.80
Slag-linecorrosion (%)	18.96 17.27	10.89 10.46	22.63 / 27.27 34.29 / 25.19
inch/h (slag-line)	0.111 0.102	0.065 0.062	0.133 / 0.162 0.193 / 0.148

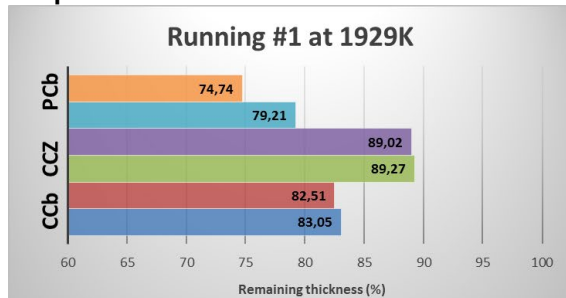
Source: Author

### 3. DISCUSSIONS

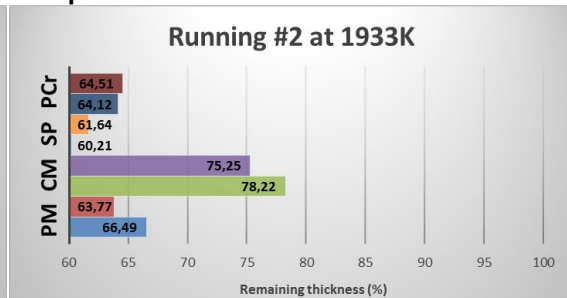
Dissolution or diffusion is a chemical process by which the refractory material is continuously dissolved or corroded into metal and metal liquid. Penetration, by which the slag penetrates into the refractory and causes mechanical effects (capillary model). Erosion is the abrasion process of the refractory material exposed to gas and slag movement<sub>Ref. (4)</sub>.

Remaining thickness were calculated to demonstrated how stable were each type of brick under investigated conditions. In general, oxide-carbons bricks kept better original shape than oxide bricks. Graphics 1, 3 and 5 show oxide carbon bricks with larger non-attacked thickness and, graphics 2,4 and 6 show oxide bricks.

**Graphic 1: Oxide-carbon bricks**

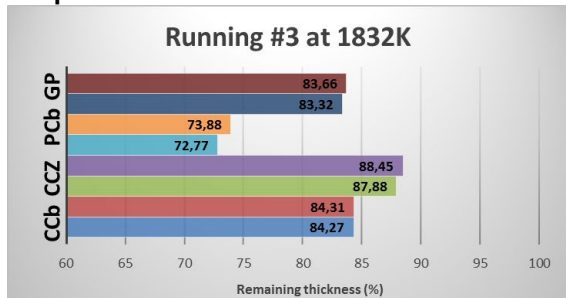


**Graphic 2: Oxide bricks**

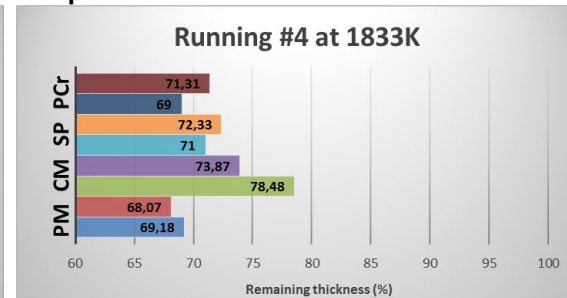


Source: Author

**Graphic 3: Oxide-carbon bricks**

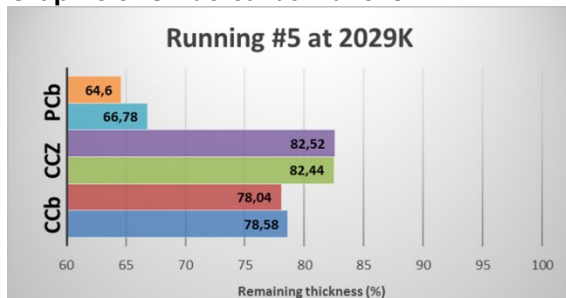


**Graphic 4: Oxide bricks**

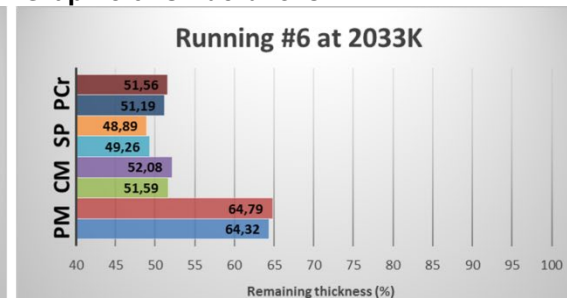


Source: Author

**Graphic 5: Oxide-carbon bricks**



**Graphic 6: Oxide bricks**



Source: Author

The results suggest better performance to the oxide-carbon group in all temperature. Further analysis shows CCZ as the best performance under investigated conditions. Among oxide bricks, CM had a spotted achievement. Basic bricks were strongly attacked by slag, even when carbon was present.

The best performance of the neutral oxide-carbon lining is in accordance with average basicity of Pyrometallurgicalconcentrate. Chemical composition on table 15 shows acid character according to Flood, H. and T. Förland<sup>Ref. (6)</sup>.

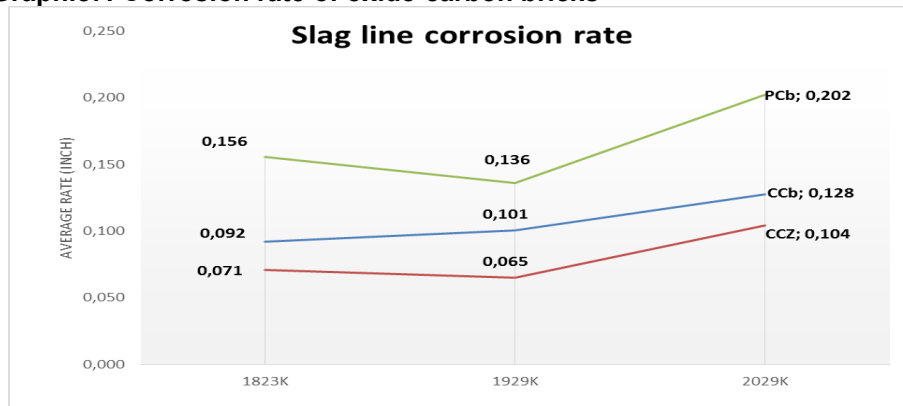
**Table 15:** Pyrometallurgicalconcentrate basicity

Typical Sample	% Nb <sub>2</sub> O <sub>5</sub>	% Fe <sub>2</sub> O <sub>3</sub>	% SiO <sub>2</sub>	% P <sub>2</sub> O <sub>5</sub>	% TiO <sub>2</sub>
Refined Concentrate	60.0 to 63.0	2.0 to 5.0	1.0 to 3.0	0.05 to 0.30	3.0 to 6.0
Character	Weaklyacid	Weaklyacid	Acid	Acid	Neutral

Source: CBMM

It had been expected that all remaining thickness and corrosion rate decreased with lower temperatures. To oxide-carbon bricks, graphic 7, the results do not follow a singular orientation. Taking in mind oxide bricks results, and multi orientation results to oxide-carbon bricks, carbon presence acted its main role.

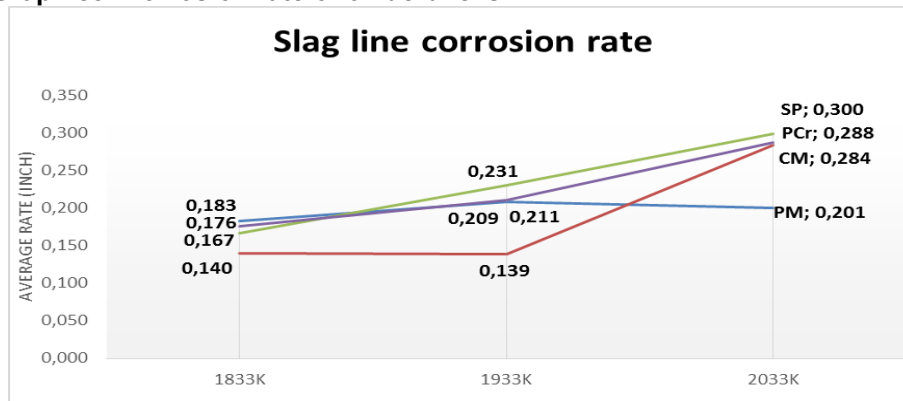
**Graphic7: Corrosion rate of oxide-carbon bricks**



Source: Author

Regarding all experiments were carried out in static conditions, higher temperatures lead to more fluid slags, with higher wettability and corrosion rates. In higher temperatures, carbon non-wettability effect seems to be more prominent. This explains why the corrosion rate increased to CCZ and PCbbricks. To PCbbrick, carbon is more important due Periclase basic character.

**Graphic8: Corrosion rate of oxide bricks**



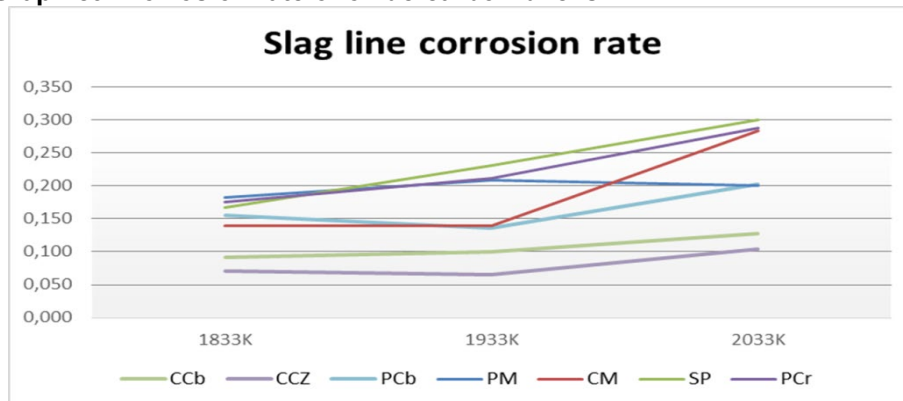
Source: Author

At 2029K, PM had a disconnected behavior, which could be related to Periclase strength in high temperature, but this result appears to be consequence of thickness measurements error.

Comparing the effect of temperature versus corrosion rates, it might be considered a direct correlation between temperature and corrosion rates. Hence, operational temperatures should be controlled ever as an important operational parameter and never as consequence of refining process.

The effect of temperature at slag working lining is expressed by graphic9.

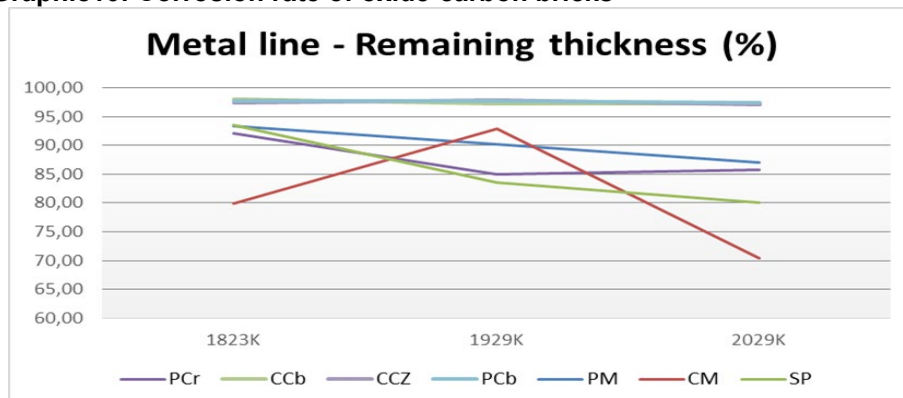
**Graphic9: Corrosion rate of oxide-carbon bricks**



Source: Author

Although slag corrosion rate is more relevant wearing mechanism for metallurgical process, it is important to analyze the effect of liquid metal on linings. Graphic 10 shows the remaining thickness of each type of brick used in this investigation. All oxide-carbon bricks kept over 95% of their original thickness in all temperatures, while oxide bricks decrease their thickness in higher temperatures. For oxide-carbon bricks does not matter what type of oxidewas used, Corundum or Periclase, because the average remaining thickness was very closed each other, 97,46% and 97,53% respectively. PM was less corroded by liquid steel among oxide bricks.

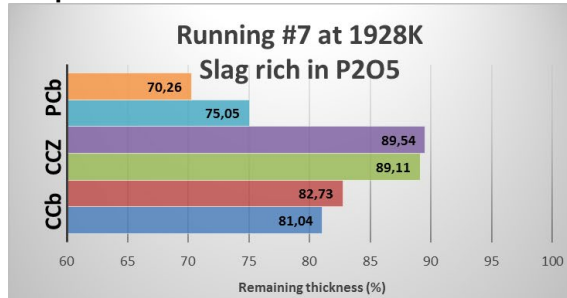
**Graphic10: Corrosion rate of oxide-carbon bricks**



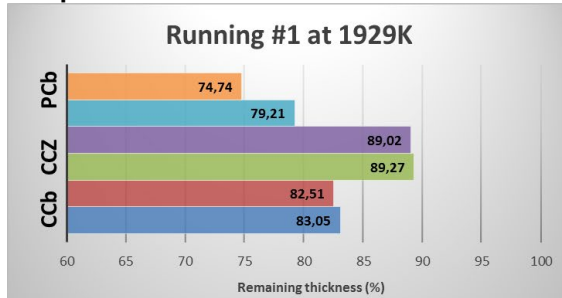
Source: Author

The effect of  $P_2O_5$  in corrosion rate is clearer to PCb than to other bricks. Roughly,  $P_2O_5$  affected negatively the refractory stability. To CCZ bricks, this effect was lower than others. Zirconia could have enhanced this stability due to its excellent resistance to chemical attack. As shown in table 15,  $P_2O_5$  is an acid compound and, PCb was more corroded, as predicted Ref. (5).

Graphic 11: Oxide-carbon bricks



Graphic 1: Oxide-carbon bricks



Source: Author

## CONCLUSIONS

The neutral group  $R_2O_3$  with carbon reported more efficient than others, even when carbon was added in these other groups.

Specimen CM has the best performance among oxide bricks, but it was severely corroded in a highest experimental temperature, confirming the remarkable action of carbon in operational process. Periclase demonstrated to be unsuitable for these conditions, especially regarding acid slag character. The same conclusion could be taken into account for bricks formed by periclase-corundum or periclase-chromia.

CCZ have presented the best performance in all experimental temperatures. Ccb reported a good performance, whilst added by zirconia this compound demonstrated an improved performance with the smallest corrosion rate. Temperature effect on slag or metal line corrosion was not impressive comparing with other materials. Whereby the distinction is the presence of zirconia, and knowing the benefits of this oxide in chemical stability, it may be concluded that zirconia is responsible for this extra performance.

Temperature is a critical parameter to Pyrometallurgical process. Higher temperatures will result in accelerated wearing, which might reach 60% upward.

Slag rich in  $P_2O_5$  is deleterious to refractory strength, but its effect seems not be immediate to lining and would be restricted by property bricks.

## ACKNOWLEDGMENTS

G.E.Gonçalves, Magnesita S.A., Contagem, MG, Brazil;  
 A.P.M. Mati, Researcher, Magnesita S.A., Contagem, MG; Brazil;  
 Eduardo Augusto Ayrosa Galvão Ribeiro, CBMM, Araxá, MG, Brazil.

## REFERENCES

- (1) Lee, W.E.; Zhang, S.; Melt Corrosion of oxide and oxide-carbon refractories; International Materials Reviews, 1999, vol. 04, n° 3.
- (2) Jones, Peter T.; Degradation Mechanisms of Basic Refractory Materials during the Secondary Refining of Stainless Steel in VOD Ladles; KatholiekeUniversiteit Leuven; Doctoral Thesis; Leuven.
- (3) Rigaud, M.; Corrosion of Refractories and Ceramics; EcolePolytechnique, Montreal, Quebec, CA; Uhlig's Corrosion Handbook, Third Edition, pag. 387 to 398.
- (4) Brosnam, Denis A.; Corrosion of refractories; Clemson University, Clemson, South Caroline, USA; pag. 39 to 49.
- (5) Wang Xiao hui, Zheng Shi li, Xu Hong-bin,Zhang Yi; Dissolution behaviours of Ta<sub>2</sub>O<sub>5</sub>, Nb<sub>2</sub>O<sub>5</sub> and their mixture in KOH and H<sub>2</sub>O system; Transactions of Nonferrous Metals Society of China.
- (6) FLOOD, H. and T. FÖRLAND (1947): The acidic and basic properties of oxides, Acta Chem. Scand., 1, 952-1005.